Porphyrinoids

International Edition: DOI: 10.1002/anie.201503530
German Edition: DOI: 10.1002/ange.201503530

β,β-Diborylated Subporphyrinato Boron(III) Complexes as Useful Synthetic Precursors**

*Masaaki Kitano, Yasuhiro Okuda, Eiji Tsurumaki, Takayuki Tanaka, Hideki Yorimitsu, and Atsuhiro Osuka**

Abstract: *Iridium-catalyzed borylation of B-aryl meso-free subporphyrinato boron(III) complexes (hereinafter referred to simply as subporphyrins) with bis(pinacolato)diboron gave 2,13-diborylated subporphyrins regioselectively, which served as promising synthetic precursors for 2,13-diarylated subporphyrins and doubly β-to-β 1,3-butadiyne-bridged subporphyrin dimers. 2,13-Diarylated subporphyrins display perturbed absorption spectra, depending upon the β-aryl substituents. Doubly 1,3-butadiyne-bridged syn and anti subporphyrin dimers thus prepared exhibit differently altered absorption spectra with split Soret-like bands, which have been accounted for in terms of exciton coupling.*

Subporphyrins are ring-contracted porphyrins possessing such intriguing characteristics as a 14π-aromatic system, bowl-shaped structures, and tunable absorption and emission properties.[1] Since the first synthesis of tribenzosubporphines in 2006,[2] various subporphyrins have been synthesized to explore their interesting optical, electronic, and structural attributes.[3,4] Despite these efforts, the development of novel synthetic methods that allow constructions of more elaborate subporphyrins still remains highly desired. In 2005, we reported iridium-catalyzed regioselective borylation of *meso*-free porphyrins at the β-positions adjacent to the free *meso*-position.[5a] This borylation has been demonstrated to be very effective, allowing the synthesis of a wide range of functional porphyrins including doubly butadiyne-bridged porphyrin dimers, singlet biradicaloid doubly linked corrole dimer, and porphyrin belts.[5] Inspired by these rich progresses, we planned to develop β,β′-diborylated subporphyrins as precursors for further fabricated subporphyrins. Herein, we report borylation reactions of *meso*-free subporphyrins.[6]

Initially, by following the synthesis used for the porphyrin borylation, a solution of *meso*-free subporphyrin **1** (Scheme 1) and bis(pinacolato)diboron ($(Bpin)_2$) in THF was refluxed for 9.5 h in the presence of a catalytic amount of [{Ir(cod)OMe}$_2$] and 4,4′-di-*tert*-butyl-2,2′-bipyridyl (dtbpy). After the usual workup, however, we obtained an intractable mixture that contained β,β′-diborylated subporphyrins bearing a O-Bpin group at the axial position as a major product (55%, ^{1}H NMR yield).[7] Since this product quickly decomposed on a silica gel column, the reaction mixture was directly subjected to reaction conditions (CuI and *N*-iodosuccinimide) that allowed the clean conversion of boronates to iodides.[8] This procedure yielded 2,13-diiodosubporphyrin **2** in 54% yield after conversion of the axial group to a methoxy group by heating in methanol. The structure of **2** has been fully characterized including its X-ray crystal analysis (Figure 1a).

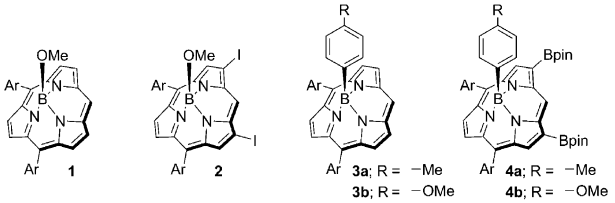

Scheme 1. Structures of subporphyrins **1**-**4**. Ar = *p*-tolyl.

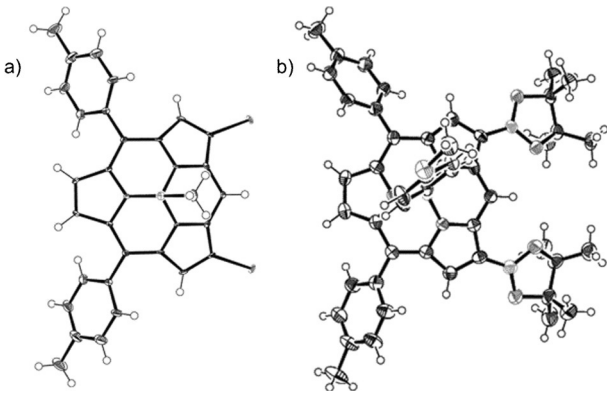

Figure 1. X-ray crystal structures of a) **2** and b) **4b**.[11,24] Ellipsoids are set at 50% probability.

These results indicated that the borylation took place with strict regioselectivity at the 2,13-positions, similarly to the borylation of *meso*-free porphyrins.

To circumvent undesired borylation at the axial position, we employed *B*-aryl *meso*-free subporphyrins **3a** and **3b** as substrates for the borylation reaction. These *B*-aryl *meso*-free subporphyrins were prepared by *B*-arylation of **1** with aryl

[*] M. Kitano, Y. Okuda, Dr. E. Tsurumaki, Dr. T. Tanaka, Prof. Dr. H. Yorimitsu, Prof. Dr. A. Osuka
Department of Chemistry, Graduate School of Science
Kyoto University, Sakyo-ku, Kyoto 606-8502 (Japan)
E-mail: osuka@kuchem.kyoto-u.ac.jp
Prof. Dr. H. Yorimitsu
ACT-C (Japan) Science and Technology Agency (Japan)

[**] This work was supported by JSPS KAKENHI Grant Numbers No. 25220802 and 25620031. M.K. acknowledges a JSPS Fellowship for Young Scientists.

Supporting information for this article is available on the WWW under http://dx.doi.org/10.1002/anie.201503530.

Grignard reagents at room temperature in the presence of trimethylsilyl chloride as an activator,[9] because when using original conditions (at reflux without activators)[10] the free *meso*-position was also arylated. Gratifyingly, the borylation of **3a** and **3b** with two equivalent amounts of $(Bpin)_2$ in the presence of a catalytic amount of $[\{Ir(cod)OMe\}_2]$ and dtbpy furnished **4a** and **4b** in 94% and 85% yields, respectively. In the crystal structure of **4b**, the two Bpin moieties are arranged nearly coplanar to the subporphyrin core, probably owing to the favorable electronic interaction between the vacant orbital of the Bpin and subporphyrin network (Figure 1b),[11] similarly to the case of diborylated porphyrins reported before.[5a]

In the next step, we examined Suzuki–Miyaura reactions of **4a** with aryl bromides (Scheme 2). After extensive screening, we found that coupling reactions of **4a** with aryl bromides using 2-dicyclohexylphosphino-2′,6′-dimethoxybiphenyl (SPhos)[12] and K_3PO_4 in THF gave 2,13-diaryl subporphyrins in moderate to good yields. Both electron-rich and -deficient aryl bromides were used, providing subporphyrins **5**, **6**, **7**, and **8** in good yields. A sterically hindered mesityl bromide was also employed to give subporphyrin **9** in moderate yield, while the use of 5-methylthien-2-yl bromide resulted in a low yield of **10**. It is worth noting that the *B*-tolyl group tolerates under the present conditions. The ^{1}H NMR spectrum of **5** exhibits a set of signals consisting of a doublet at 8.05 ppm and triplets at 7.58 and 7.46 ppm that are due to the β-phenyl groups, indicating their free rotation. In contrast, the ^{1}H NMR spectrum of **9** taken at room temperature shows two sets of signals due to the *ortho*-methyl protons and *meta*-aryl protons of the β-mesityl groups, indicating their restricted rotations.[13]

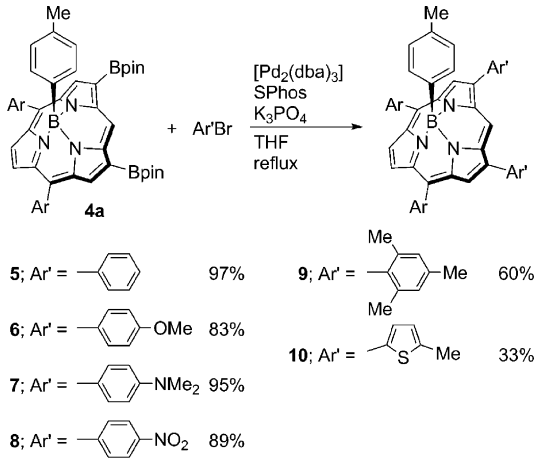

Scheme 2. Suzuki–Miyaura reactions of subporphyrin **4a**. Ar = *p*-tolyl.

The UV/Vis absorption and fluorescence spectra of **3a** and **5**–**10** in CH_2Cl_2 are shown in Figure 2. Compared with β-unsubstituted subporphyrin **3a**, 2,13-diphenylated subporphyrin **5** shows a red-shifted Soret-like band at 395 nm, indicating effective electronic interaction between the subporphyrin and β-phenyl substituents. Introduction of electron-donating and -withdrawing substituents at the *para*-position of the β-aryl substituents leads to perturbation of the photophysical properties of subporphyrins. 2,13-Bis(4-nitrophenyl)subporphyrin **8** shows a significantly red-shifted Soret-like band at 419 nm and Q-like bands at 489 and 523 nm, while 2,13-bis(4-dimethylaminophenyl)subporphyrin **7** displays a characteristically broad and split Soret-like band, similar to the previously reported *meso*-(4-aminophenyl)-substituted[3b] and β-arylamino-substituted[14] subporphyrins. On the other hand, only small red-shifts was observed in the absorption spectrum of bis-2,4,6-trimethylphenyl-substituted subporphyrin **9**, which is probably due to the sterically congested β-aryl substituents. The Soret-like band of 5-methylthienylated subporphyrin **10** is most broadened, reflecting the presence of a wider range of conformers with regard to the β-(5-methylthien-2-yl) substituents. Here, it is worth noting that β,β-diarylated porphyrins show much less influences on their optical properties.[15]

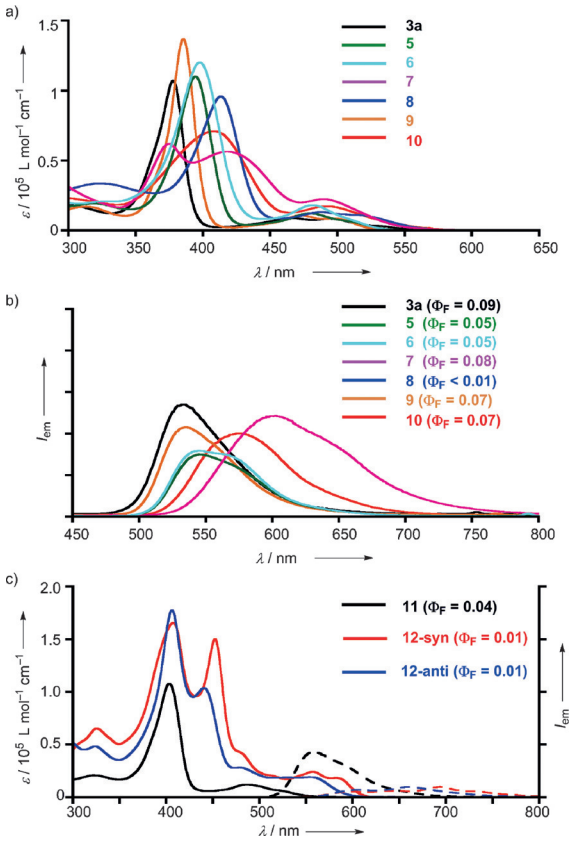

Figure 2. a) UV/Vis absorption and b) fluorescence spectra of subporphyrins **3a** and **5**–**10** in CH_2Cl_2 and c) UV/Vis absorption (——) and fluorescence (-----) spectra of subporphyrins **11**, **12**-*syn*, and **12**-*anti* in CH_2Cl_2.

Subporphyrin **3a** exhibits fluorescence at 534 nm with $\Phi_F = 0.09$. Subporphyrins **5**, **6**, and **9** show similar fluorescence at 545 nm ($\Phi_F = 0.05$), 544 nm ($\Phi_F = 0.05$), and 536 nm ($\Phi_F = 0.07$), respectively. On the other hand, subporphyrins **7** and **10** possessing electron-donating β-aryl substituents show red-shifted fluorescence spectra at 603 nm ($\Phi_F = 0.08$) and at 576 nm ($\Phi_F = 0.07$), respectively. Subporphyrin **8** is practically non-fluorescent, probably owing to fast intramolecular electron transfer in the excited state.[6,16]

Electrochemical properties were examined by cyclic voltammetry (CV) in CH_2Cl_2 containing Bu_4NPF_6 (0.1M) as a supporting electrolyte (Supporting Information, Figure S7-1). The first oxidation and reduction potentials were observed as reversible waves at 0.62 and −1.94 V for **5**, 0.58 and −1.98 V for **6**, and 0.60 and −2.07 V for **9**, respectively, which are higher than those of **3a** (0.50 and −2.13 V). Subporphyrin **7** showed a negatively shifted oxidation potential at 0.26 V and subporphyrin **8** showed a positively shifted reduction potential at −1.49 V, which have been assigned respectively to the oxidation of the 4-dimethylaminophenyl group and reduction of the 4-nitrophenyl group. A plot of the first redox potentials of **5**–**8** except for oxidation of **7** or reduction of **8** versus the Hammet σ constant of *para*-substituents on β-aryl rings has a good straight-line fit with a slope $\rho = 0.059$ V for oxidation and 0.071 V for reduction potentials (Supporting Information, Figure S7-2).

DFT calculations were performed at the B3LYP/6-311G(d) level using the Gaussian 09 package. The calculated four frontier orbitals of **3a** reveal porphyrin-like orbital shapes,[17] among which LUMO+1 and HOMO−1 have large electron coefficients at the 2,13-positions (Supporting Information, Figure S5-1). Both HOMO and HOMO−1 of **3a** are energetically close to HOMO of aniline molecule, but HOMO−1 that possesses large electron coefficients at the 2,13-positions can be better interacted with HOMO of aniline moiety in **7** (Supporting Information, Figure S5-2). This situation may explain the observed split Soret-like band of **7**. Similarly, effective orbital–orbital interaction between LUMO+1 of **3a** and LUMO of the nitrophenyl groups causes perturbed LUMO and LUMO+3 of 4-nitrophenyl substituted subporphyrin **8**, which explains it having the smallest HOMO–LUMO gap.

In the next step, 2,13-diborylated subporphyrin **4b** was used for synthesis of doubly β-to-β 1,3-butadiyne-bridged subporphyrin dimers (Scheme 3). 2,13-Bis-(*tert*-butyldimethylsilylethynyl)subporphyrin **11** was prepared in 85% yield by a cross-coupling reaction of **4b** with 1-bromo-2-(*tert*-butyldimethylsilyl)acetylene under the reaction conditions used for the Suzuki–Miyaura coupling described above. After deprotection of the silyl groups, $Cu(OAc)_2$-mediated dimerization[18] of **11** furnished β-to-β 1,3-butadiyne-bridged subporphyrin dimers **12**-*syn* and **12**-*anti* in 30% and 28% yields, respectively. The structures of **12**-*syn* and **12**-*anti* have been confirmed by X-ray structural analysis (Figure 3).[19] Averaged bond angles of $C(sp^2)-C_\alpha\equiv C_\beta$ and $C_\alpha\equiv C_\beta-C_{\beta'}$ (θ_1 and θ_2) of four non-equivalent C≡C units are 170.4 and 174.2° for **12**-*syn* and 170.5 and 175.4° for **12**-*anti,* indicating distortions of the triple bonds in **12**-*syn* and **12**-*anti*, which are larger than those of the doubly butadiyne-bridged porphyrin dimer (174.6 and 177.9°).[18a] Average bond length of $C(sp^2)-C_\alpha$, $C_\alpha-C_\beta$, and $C_\beta-C_{\beta'}$ are 1.42, 1.20, and 1.38 Å for **12**-*syn*, respectively, and 1.42, 1.21, and 1.37 Å for **12**-*anti*, respectively, indicating no substantial differences between the two conformers. These structural data indicated small structural distortions around the double 1,3-butadiynyl bridges. On the other hand, averaged bowl depths of the subporphyrin cores are 1.46 Å for **12**-*syn* and 1.50 Å for **12**-*anti*,[20] and center-to-center distances (B–B distance) are 11.92 Å for **12**-*syn* and 11.97 Å for **12**-*anti*, showing slightly but distinct differences between the two isomers. In ^{1}H NMR spectra, singlet signals due to the free *meso*-positions are observed at $\delta = 10.20$ ppm and 9.74 ppm for **12**-*syn* and **12**-*anti*, respectively, which has been ascribed to larger influence of the anisotropic effect of the butadiyne moieties in the former as compared with the latter. More importantly, these two isomers have different orientation of the two subporphyrin units, which leads to different exciton coupling as discussed below.

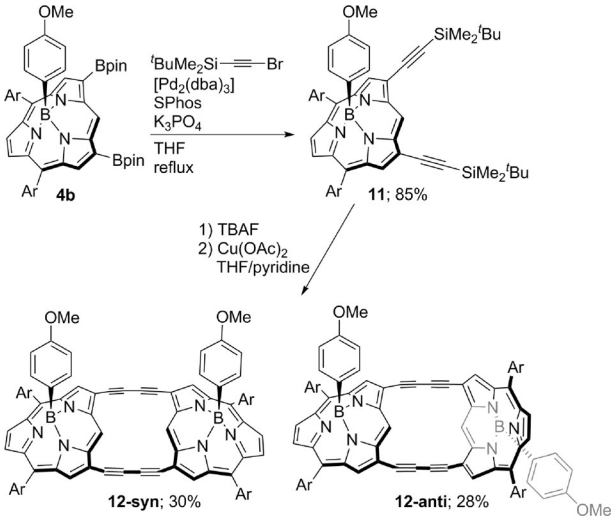

Scheme 3. Synthesis of β-to-β 1,3-butadiyne-bridged subporphyrin dimers **12**-*syn* and **12**-*anti*. Ar = *p*-tolyl.

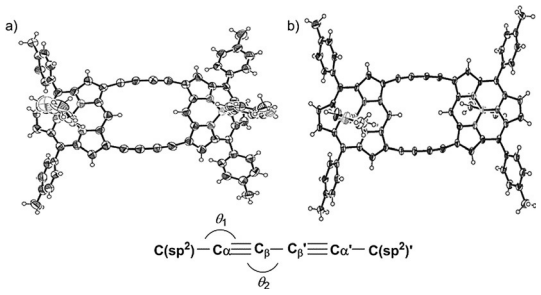

Figure 3. X-ray crystal structures of a) **12**-*syn* and b) **12**-*anti*.[19,24] Solvent molecules are omitted for clarity, and ellipsoids are set at 50% probability.

2,13-Diethynylsubporphyrin **11** shows a Soret-like band at 404 nm and a Q-like band at 487 nm, both of which are considerably red-shifted as compared with **3b** (Figure 2c). Both dimers **12**-*syn* and **12**-*anti* exhibit split Soret-like bands at 409 and 453 nm and at 406 and 441 nm,[21] and more red-shifted Q-like bands at 557 and 583 nm and at 554 nm, respectively, indicating large electronic coupling of the two subporphyrins and a significant difference in the absorption spectra of the two isomers. The observed split Soret-like bands of **12**-*syn* and **12**-*anti* have been deconvoluted into three and two Cauchy-Lorentz distribution functions at 401, 410, and 452 nm and at 405 and 443 nm, respectively, by least-square curve fitting (Supporting Information, Figure S4-2).

These deconvoluted absorption spectra can be qualitatively explained in terms of exciton coupling using dipole–dipole approximation developed by Kasha,[22] where two transition dipole moments are placed parallel (**A** and **A′**) and perpendicular (**B**) to the short molecular axis (Supporting Information, Figure S4-3). The parallel dipoles (**A** and **A′**) of **12**-*syn* and **12**-*anti* are interacted each other to allow only blue-shifted transitions. Calculated splitting energy ΔE_A estimated from the crystal structure of **12**-*syn* is slightly larger than that of **12**-*anti*, which corresponds to 401 nm peak of **12**-*syn* and to 405 nm peak of **12**-*anti*.[23a] On the other hand, the perpendicular dipoles (**B** and **B′**) of **12**-*syn* are arranged in an oblique arrangement, while those in **12**-*anti* are arranged in a parallel arrangement. In both cases, red-shifted transitions are allowed, and the splitting energy ΔE_B was calculated to be larger for **12**-*syn* compared with that of **12**-*anti*.[23b] These calculations explain well the observed spectra of **12**-*syn* and **12**-*anti* (Supporting Information). The fluorescence spectra of **12**-*syn* (694 nm, $\Phi_F = 0.01$) and **12**-*anti* (660 nm, $\Phi_F = 0.01$) are significantly red-shifted as compared with that of **11** (558 nm, $\Phi_F = 0.04$).

In summary, Ir-catalyzed borylation with $(Bpin)_2$ has been demonstrated to be effective for *B*-aryl *meso*-free subporphyrins, producing 2,13-diborylated subporphyrins regioselectively in good yields. The diborylated subporphyrins thus prepared were used for the synthesis of 2,13-diarylated *B*-aryl subporphyrins and doubly β-to-β 1,3-butadiyne-bridged subporphyrin dimers. 2,13-Diarylated subporphyrins display altered absorption spectra, depending upon the β-aryl substituents. Doubly 1,3-butadiyne-bridged subporphyrin dimers (**12**-*syn* and **12**-*anti*) exhibit substantially perturbed absorption spectra with split Soret-like bands, which can be accounted for in terms of exciton coupling. Applications of β-borylated subporphyrins for exploration of more elaborated functional subporphyrin oligomers are actively in progress in our laboratory.

Keywords: borylation · cross-coupling · exciton coupling · porphyrinoids · subporphyrins

How to cite: *Angew. Chem. Int. Ed.* **2015**, *54*, 9275–9279
Angew. Chem. **2015**, *127*, 9407–9411

[1] a) Y. Inokuma, A. Osuka, *Dalton Trans.* **2008**, 2517; b) T. Torres, *Angew. Chem. Int. Ed.* **2006**, *45*, 2834; *Angew. Chem.* **2006**, *118*, 2900; c) A. Osuka, E. Tsurumaki, T. Tanaka, *Bull. Chem. Soc. Jpn.* **2011**, *84*, 679; d) C. G. Claessens, D. González-Rodríguez, M. S. Rodríguez-Morgade, A. Medina, T. Torres, *Chem. Rev.* **2014**, *114*, 2192.

[2] a) Y. Inokuma, J. H. Kwon, T. K. Ahn, M.-C. Yoo, D. Kim, A. Osuka, *Angew. Chem. Int. Ed.* **2006**, *45*, 961; *Angew. Chem.* **2006**, *118*, 975.

[3] a) Y. Inokuma, S. Easwaramoorthi, S. Y. Jang, K. S. Kim, D. Kim, A. Osuka, *Angew. Chem. Int. Ed.* **2008**, *47*, 4840; *Angew. Chem.* **2008**, *120*, 4918; b) Y. Inokuma, S. Easwaramoorthi, Z. S. Yoon, D. Kim, A. Osuka, *J. Am. Chem. Soc.* **2008**, *130*, 12234; c) Y. Inokuma, Z. S. Yoon, D. Kim, A. Osuka, *J. Am. Chem. Soc.* **2007**, *129*, 4747; d) N. Kobayashi, Y. Takeuchi, A. Matsuda, *Angew. Chem. Int. Ed.* **2007**, *46*, 758; *Angew. Chem.* **2007**, *119*, 772; e) Y. Takeuchi, A. Matsuda, N. Kobayashi, *J. Am. Chem. Soc.* **2007**, *129*, 8271.

[4] Selected examples for related free-base ring-contracted porphyrins: a) R. Myśliborski, L. Latos-Grażyński, L. Szterenberg, T. Lis, *Angew. Chem. Int. Ed.* **2006**, *45*, 3670; *Angew. Chem.* **2006**, *118*, 3752; b) Z. Xue, Z. Shen, J. Mack, D. Kuzuhara, H. Yamada, T. Okujima, N. Ono, X.-Z. You, N. Kobayashi, *J. Am. Chem. Soc.* **2008**, *130*, 16478.

[5] a) H. Hata, H. Shinokubo, A. Osuka, *J. Am. Chem. Soc.* **2005**, *127*, 8264; b) S. Hiroto, K. Furukawa, H. Shinokubo, A. Osuka, *J. Am. Chem. Soc.* **2006**, *128*, 12380; c) S. Yamaguchi, T. Katoh, H. Shinokubo, A. Osuka, *J. Am. Chem. Soc.* **2007**, *129*, 6392; d) J. Song, S. Y. Jang, S. Yamaguchi, J. Sankar, S. Hiroto, N. Aratani, J.-Y. Shin, S. Easwaramoorthi, K. S. Kim, D. Kim, H. Shinokubo, A. Osuka, *Angew. Chem. Int. Ed.* **2008**, *47*, 6004; *Angew. Chem.* **2008**, *120*, 6093; e) S. Hiroto, I. Hisaki, H. Shinokubo, A. Osuka, *J. Am. Chem. Soc.* **2008**, *130*, 16172; f) J. Song, N. Aratani, P. Kim, D. Kim, H. Shinokubo, A. Osuka, *Angew. Chem. Int. Ed.* **2010**, *49*, 3617; *Angew. Chem.* **2010**, *122*, 3699; g) J. Song, N. Aratani, J. H. Heo, D. Kim, H. Shinokubo, A. Osuka, *J. Am. Chem. Soc.* **2010**, *132*, 11868; h) J. Song, N. Aratani, H. Shinokubo, A. Osuka, *J. Am. Chem. Soc.* **2010**, *132*, 16356.

[6] a) M. Kitano, S. Hayashi, T. Tanaka, H. Yorimitsu, N. Aratani, A. Osuka, *Angew. Chem. Int. Ed.* **2012**, *51*, 5593; *Angew. Chem.* **2012**, *124*, 5691; b) M. Kitano, J. Sung, K. H. Park, H. Yorimitsu, D. Kim, A. Osuka, *Chem. Eur. J.* **2013**, *19*, 16523.

[7] The major product was assumed to be **s2** (see the Supporting Information), which shows the ^{1}H NMR peak of the B−OBpin group at 0.64 ppm and the HRMS spectrum at *m*/*z* 817.4468 (calcd for $C_{47}H_{55}{}^{11}B_4N_3O_7 = 817.4435$ [**s2**]$^+$).

[8] a) J. M. Murphy, X. Liao, J. F. Hartwig, *J. Am. Chem. Soc.* **2007**, *129*, 15434; b) H. Wu, J. Hynes, Jr., *Org. Lett.* **2010**, *12*, 1192; c) J. F. Hartwig, *Acc. Chem. Res.* **2012**, *45*, 864; d) B. M. Partridge, J. F. Hartwig, *Org. Lett.* **2013**, *15*, 140; e) P. S. Fier, J. Luo, J. F. Hartwig, *J. Am. Chem. Soc.* **2013**, *135*, 2552; f) K. Fujimoto, H. Yorimitsu, A. Osuka, *Org. Lett.* **2014**, *16*, 972.

[9] J. Guilleme, D. González-Rodríguez, T. Torres, *Angew. Chem. Int. Ed.* **2011**, *50*, 3506; *Angew. Chem.* **2011**, *123*, 3568.

[10] a) E. Tsurumaki, S. Hayashi, F. S. Tham, C. A. Reed, A. Osuka, *J. Am. Chem. Soc.* **2011**, *133*, 11956; b) S. Saga, S. Hayashi, K. Yoshida, E. Tsurumaki, P. Kim, Y. M. Sung, J. Sung, T. Tanaka, D. Kim, A. Osuka, *Chem. Eur. J.* **2013**, *19*, 11158.

[11] Crystal data for **2**: $C_{15}H_{11}B_{0.5}N_{1.5}I$, $M_w = 352.56$, orthorhombic, space group $Cmc2_1$ (No.36), $a = 27.651(7)$, $b = 11.974(4)$, $c = 7.881(2)$ Å, $V = 2609.4(13)$ Å^3, $T = 93$ K, $\rho_{calcd} = 1.795$ g cm^{-3}, $Z = 8$, $R_1 = 0.0659$ [$I > 2.0\sigma(I)$], $wR_2 = 0.1702$ (all data), GOF = 1.056. Crystal data for **4b**: $C_{48}H_{50}B_3N_3O_5$, $M_w = 781.34$, orthorhombic, space group $Pca2_1$ (No.29), $a = 20.968(5)$, $b = 15.562(4)$, $c = 12.909(3)$ Å, $V = 4212.2(18)$ Å^3, $T = 93$ K, $\rho_{calcd} = 1.232$ g cm^{-3}, $Z = 4$, $R_1 = 0.0646$ [$I > 2.0\sigma(I)$], $wR_2 = 0.1728$ (all data), GOF = 1.037.

[12] T. E. Barder, S. D. Walker, J. R. Martinelli, S. L. Buchwald, *J. Am. Chem. Soc.* **2005**, *127*, 4685.

[13] K. Yoshida, G. Copley, H. Mori, A. Osuka, *Chem. Eur. J.* **2014**, *20*, 10065.

[14] a) E. Tsurumaki, A. Osuka, *Chem. Asian J.* **2013**, *8*, 3042; b) S. Easwaramoorthi, J.-Y. Shin, S. Cho, P. Kim, Y. Inokuma, E. Tsurumaki, A. Osuka, D. Kim, *Chem. Eur. J.* **2009**, *15*, 12005.

[15] Y. Kawamata, S. Tokuji, H. Yorimitsu, A. Osuka, *Angew. Chem. Int. Ed.* **2011**, *50*, 8867; *Angew. Chem.* **2011**, *123*, 9029.

[16] W.-Y. Cha, J. M. Lim, K. H. Park, M. Kitano, A. Osuka, D. Kim, *Chem. Commun.* **2014**, *50*, 8491.

[17] M. Gouterman, *J. Mol. Spectrosc.* **1961**, *6*, 138.

[18] a) I. Hisaki, S. Hiroto, K. S. Kim, S. B. Noh, D. Kim, H. Shinokubo, A. Osuka, *Angew. Chem. Int. Ed.* **2007**, *46*, 5125; *Angew. Chem.* **2007**, *119*, 5217; b) S. Tokuji, H. Yorimitsu, A. Osuka, *Angew. Chem. Int. Ed.* **2012**, *51*, 12357; *Angew. Chem.* **2012**, *124*, 12523.

[19] Crystal data for **12**-*syn*: $C_{80}H_{52}B_2N_6O_2 \cdot 1.5$(toluene), $M_w =$ 1289.10, triclinic, space group $P\bar{1}$ (No.2), $a = 11.728(16)$, $b =$ 14.923(18), $c = 20.72(2)$ Å, $\alpha = 96.8020(9)$, $\beta = 97.35(5)$, $\gamma =$ 108.81(2)°, $V = 3354(7)$ Å^3, $T = 93$ K, $\rho_{calcd} = 1.276$ g cm^{-3}, $Z = 2$, $R_1 = 0.1198$ [$I > 2.0\sigma(I)$], $wR_2 = 0.3955$ (all data), GOF = 1.062. Crystal data for **12**-*anti*: $C_{80}H_{52}B_2N_6O_2 \cdot 3$(toluene), $M_w =$ 1411.17, triclinic, space group $P\bar{1}$ (No.2), $a = 16.0080(6)$, $b =$ 17.333(2), $c = 17.832(4)$ Å, $\alpha = 61.20(6)$, $\beta = 64.85(5)$, $\gamma =$ 72.22(6)°, $V = 3893.2(9)$ Å^3, $T = 93$ K, $\rho_{calcd} = 1.204$ g cm^{-3}, $Z =$ 2, $R_1 = 0.0803$ [$I > 2.0\sigma(I)$], $wR_2 = 0.3112$ (all data), GOF = 1.078.

[20] The bowl depth is defined as the distance from the mean plane of the peripheral six β-carbons to the center boron atom.

[21] Similar photophysical features including split Soret-bands have been reported for covalently-linked porphyrin dimers; a) J. P. Collman, C. M. Elliott, T. R. Halbert, B. S. Tovrog, *Proc. Natl. Acad. Sci. USA* **1977**, *74*, 18; b) J. B. Paine III, D. Dolphin, M. Gouterman, *Can. J. Chem.* **1978**, *56*, 1712; c) A. Osuka, K. Maruyama, *J. Am. Chem. Soc.* **1988**, *110*, 4454.

[22] M. Kasha, H. R. Rawls, M. A. El-Bayoumi, *Pure Appl. Chem.* **1965**, *11*, 371.

[23] a) ΔE_A values have been calculated to be $1.67 \times 10^{21} |\boldsymbol{M}_A|^2$ and $1.55 \times 10^{21} |\boldsymbol{M}_A|^2 \text{cm}^{-3}$ for **12**-*syn* and **12**-*anti*, respectively; b) ΔE_B values have been calculated to be $3.03 \times 10^{21} |\boldsymbol{M}_B|^2$ and $2.47 \times 10^{21} |\boldsymbol{M}_B|^2 \text{cm}^{-3}$ for **12**-*syn* and **12**-*anti*, respectively (see the Supporting Information, Figure S4-4).

[24] CCDC 1054655 (**2**), CCDC 992386 (**4b**), CCDC 992388 (**12**-*syn*), and CCDC 992387 (**12**-*anti*) contain the supplementary crystallographic data for this paper. These data are provided free of charge by The Cambridge Crystallographic Data Centre.

Received: April 18, 2015
Published online: June 18, 2015

